The emergence of longevous populations

Fernando Colchero[a,b,c], Roland Rau[c,d], Owen R. Jones[a,e], Julia A. Barthold[a,f], Dalia A. Conde[a,e], Adam Lenart[a,f], Laszlo Nemeth[c], Alexander Scheuerlein[c], Jonas Schoeley[a,c,f], Catalina Torres[a,f], Virginia Zarulli[a,f], Jeanne Altmann[g,h], Diane K. Brockman[i], Anne M. Bronikowski[j], Linda M. Fedigan[k], Anne E. Pusey[l], Tara S. Stoinski[m], Karen B. Strier[n], Annette Baudisch[a,e,f], Susan C. Alberts[h,l,o,p,1], and James W. Vaupel[a,c,f,p,1]

[a]Max-Planck Odense Center on the Biodemography of Aging, University of Southern Denmark, Odense 5230, Denmark; [b]Department of Mathematics and Computer Science, University of Southern Denmark, Odense 5230, Denmark; [c]Max Planck Institute for Demographic Research, Rostock 18057, Germany; [d]Institute of Sociology and Demography, University of Rostock, Rostock 18057, Germany; [e]Department of Biology, University of Southern Denmark, Odense 5230, Denmark; [f]Department of Public Health, University of Southern Denmark, Odense 5000, Denmark; [g]Department of Ecology and Evolutionary Biology, Princeton University, Princeton, NJ 08544; [h]Institute of Primate Research, National Museums of Kenya, 00502 Nairobi, Kenya; [i]Department of Anthropology, University of North Carolina, Charlotte, NC 28223; [j]Department of Ecology, Evolution, and Organismal Biology, Iowa State University, Ames, IA 50011; [k]Department of Anthropology and Archaeology, University of Calgary, Calgary, AB, Canada T2N 1N4; [l]Department of Evolutionary Anthropology, Duke University, Durham, NC 27708; [m]The Dian Fossey Gorilla Fund International and Zoo Atlanta, Atlanta, GA 30315; [n]Department of Anthropology, University of Wisconsin, Madison, WI 53706; [o]Department of Biology, Duke University, Durham, NC 27708; and [p]Duke Population Research Institute, Duke University, Durham, NC 27708

Contributed by James W. Vaupel, October 17, 2016 (sent for review July 26, 2016; reviewed by Michael Murphy and Deborah Roach)

The human lifespan has traversed a long evolutionary and historical path, from short-lived primate ancestors to contemporary Japan, Sweden, and other longevity frontrunners. Analyzing this trajectory is crucial for understanding biological and sociocultural processes that determine the span of life. Here we reveal a fundamental regularity. Two straight lines describe the joint rise of life expectancy and lifespan equality: one for primates and the second one over the full range of human experience from average lifespans as low as 2 y during mortality crises to more than 87 y for Japanese women today. Across the primate order and across human populations, the lives of females tend to be longer and less variable than the lives of males, suggesting deep evolutionary roots to the male disadvantage. Our findings cast fresh light on primate evolution and human history, opening directions for research on inequality, sociality, and aging.

biodemography | equality | lifespan | pace and shape | senescence

Longevous populations have two characteristics: The average length of life is long and relative variation in lifespans is low. For example, life tables for contemporary Sweden and Japan indicate that most deaths occur at ages between the late 70s and early 90s. Our primate relatives, in contrast, have lifespans that are highly variable in length but short on average and rarely longer than 30 y (Fig. 1). An association between the average length of life and its variability has been found for industrialized societies (1, 2). However, detailed knowledge is lacking about whether and how this association varies across species separated by millions of years of primate evolution or whether it has changed over the past several centuries of unprecedented social progress in human populations. Fuller comprehension of the relationship between rising lifespans and reduced lifespan variability across evolution and history holds potential insights that might illuminate past, current, and future longevity.

We pose three related questions aimed at filling this knowledge gap: How long and variable are lifespans for humans compared with nonhuman primates, for humans today compared with the past, and for males compared with females? We provide answers to these questions by applying a powerful framework that simultaneously examines changes in both the average length of life in a population or species—the "pace" of life—and relative variation in the length of life, i.e., the "shape" of the distribution of ages at death (3–5). Studying variation in lifespan links to increasing interest in social, economic, and health inequalities and to key sociological findings that relate social factors—including high social status and social integration—to longer, healthier lifespans in human and animal societies (6–10).

Estimating the average length of life (here measured by life expectancy, the mean age at death) and variation in lifespans relative to the average (measured here as "lifespan equality"; Box 1) requires data on the ages at death of individuals. We examined lifespan distributions for six nonhuman primate populations representing species that span the primate order and for six populations of humans that represent the full range of human experience. The nonhuman primate data, collected with sustained effort and extraordinary dedication from wild populations that have been under continuous observation for between 31 y and 52 y (11, 12), include one Indriid (a lemur-like Madagascan primate), two New World monkeys, one Old World monkey, and two great apes (Table 1). These wild populations all experience natural dispersal patterns; hence, we extended Bayesian methods to estimate age-specific mortality trajectories for males and females from censored and truncated data while accounting for out-migration from the study area (13, 14) (*Materials and Methods*). Human hunter-gatherer data were drawn from published information on two populations, the Hadza and Ache (15, 16),

Significance

Public interest in social and economic equality is burgeoning. We examine a related phenomenon, lifespan equality, using data from charismatic primate populations and diverse human populations. Our study reveals three key findings. First, lifespan equality rises in lockstep with life expectancy, across primate species separated by millions of years of evolution and over hundreds of years of human social progress. Second, industrial humans differ more from nonindustrial humans in these measures than nonindustrial humans do from other primates. Third, in spite of the astonishing progress humans have made in lengthening the lifespan, a male disadvantage in lifespan measures has remained substantial—a result that will resonate with enduring public interest in male–female differences in many facets of life.

Author contributions: S.C.A. and J.W.V. designed research; F.C., R.R., A.B., S.C.A., and J.W.V. performed research; F.C., J.A.B., and A.B. contributed new reagents/analytic tools; F.C., R.R., O.R.J., J.A.B., A.L., L.N., A.S., J.S., C.T., and V.Z. analyzed data; J.A., D.K.B., A.M.B., L.M.F., A.E.P., T.S.S., K.B.S., and S.C.A. provided long-term data; and F.C., D.A.C., A.B., S.C.A., and J.W.V. wrote the paper.

Reviewers: M.M., London School of Economics; and D.R., University of Virginia.

The authors declare no conflict of interest.

Freely available online through the PNAS open access option.

Data deposition: The data used in this paper are available from the following websites: nonhuman primate data, http://datadryad.org/resource/doi:10.5061/dryad.v28t5; human life tables, www.mortality.org/; nonhuman life tables, www.demogr.mpg.de/en/laboratories/evolutionary_biodemography_1171/projects/datlife_the_demography_of_aging_across_the_tree_of_life_database_744.htm.

[1]To whom correspondence may be addressed. Email: jvaupel@health.sdu.dk or alberts@duke.edu.

This article contains supporting information online at www.pnas.org/lookup/suppl/doi:10.1073/pnas.1612191113/-/DCSupplemental.

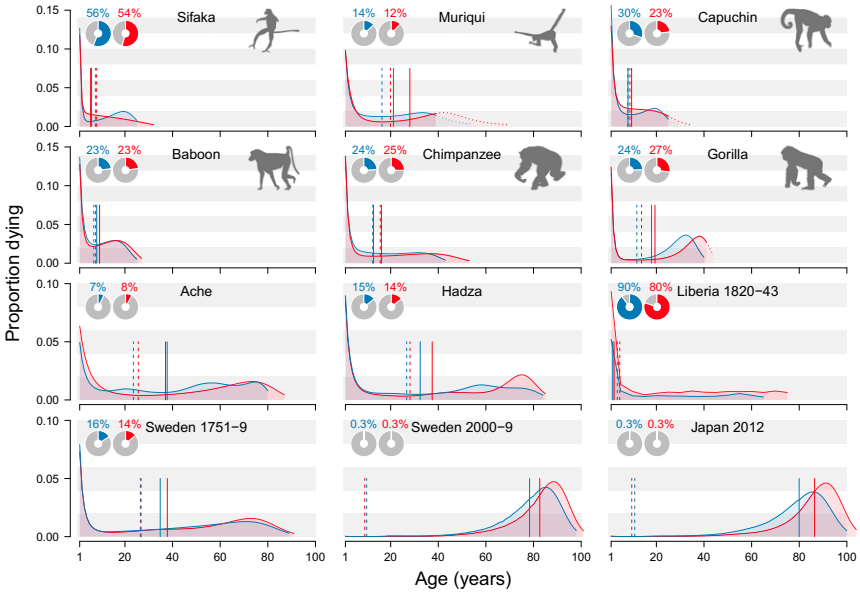

Fig. 1. Lifespan distributions for males and females. Each panel presents the proportion of individuals dying by age for females (red) and males (blue). Infant mortality (before age 1 y) is reported in *Inset* pie charts. The solid vertical lines mark life expectancies for each sex. The dashed vertical lines indicate the average number of years of life expectancy lost due to death. Keyfitz's entropy is given by this value divided by life expectancy (Box 1). For the muriqui, capuchin, and female gorillas, the curves are extrapolated beyond maximum estimated lifespans within the dataset, as indicated by dotted curves and diagonal shading (*Materials and Methods*).

that were studied carefully over many years. We also included mortality data from a human population with serviceable records and an extraordinarily low life expectancy of 2 y, namely the population of freed US slaves that emigrated to Liberia from 1820 to 1843 (17, 18). Finally, we extracted life tables from the *Human Mortality Database* (19) for Sweden in 1751–1759, Sweden in 2000–2009, and Japan in 2012 (see Table 3).

Our data reveal key common features shared by all 12 of these populations (Fig. 1). After a mortality hump in infancy (barely evident in 21st-century Japan and Sweden), the proportion dying declines with age and then generally rises again in an old-age mortality hump. The intensity of mortality before age 1 y, however, varies greatly across populations and species, from more than 80% for Liberia in 1820–1843 and 50% for the sifaka population to less than 1% for the 21st-century Swedes and Japanese (pie-chart *Insets*, Fig. 1 and Fig. S1). The two 21st-century human populations enjoy an extended period of low mortality up to old ages, when most deaths occur. Females tend to live longer than males: For most of the populations female life expectancy is higher than the male value and the oldest individuals tend to be females.

Measures of Length of Life and Lifespan Equality

The diverse mortality patterns in Fig. 1 can be summarized by population measures of (*i*) the length of life (pace) and (*ii*) relative variation in the length of life (shape).

The length of life can be captured by life expectancy, remaining life expectancy at maturity, the age that only 5% of individuals reach, and other measures (4) (*Materials and Methods* and Table S1). These measures are highly correlated with each other in the 12 populations we studied (Figs. 2 and 3 and Table 2), indicating that they cluster similarly along the slow–fast life-history continuum that has been described for mammals, birds, and some other taxa (20). Hence we chose life expectancy—the most common and theoretically most desirable measure for the pace–shape framework (4)—for further analysis.

Relative variation in the length of life can be captured by measuring the proportion that survive to maturity and by life expectancy as a proportion of the age that only 5% attain. More sophisticated statistics can be based on the coefficient of variation, the Gini coefficient, or Keyfitz's entropy (Box 1, *Materials and Methods*, Figs. 2 and 3, and Table S2), all of which are measures of how spread out a death distribution is compared with its average value: They are dimensionless measures of the shape of the distribution of lifespans. Based on a study of the properties of shape measures (5) we chose to work with a measure we call lifespan equality, which is related to Keyfitz's entropy, a measure that has proved useful in demographic analyses (21) (Box 1). Note that we do not use equality in the normative sense of fairness or justice. Although ages at death are partially shaped by social and economic inequalities, we simply use lifespan equality as a descriptive measure of the shape of the distribution of lifespans. Various measures of shape (relative lifespan variation), like the measures of pace (length of life), are highly correlated with each other, providing cogent evidence that in addition to the fast/slow continuum of the pace of life, there is

Table 1. Nonhuman primate species included in the study, showing ages at sexual maturity for each sex and the numbers of individuals for each sex for each study population

				Age at adulthood, y		Sample size by sex		
Common name	Species	Family	Country	Female	Male	Female	Male	Unknown
Sifaka	*Propithecus verreauxi*	Indriidae	Madagascar	6.5	5.5	266	342	385
Northern muriqui	*Brachyteles hypoxanthus*	Atelidae	Brazil	8.5	6.5	263	263	5
Capuchin	*Cebus capucinus*	Cebidae	Costa Rica	6.5	6.5	113	158	16
Yellow baboon	*Papio cynocephalus*	Cercopithecidae	Kenya	5.5	7.5	618	706	0
Chimpanzee	*Pan troglodytes*	Hominidae	Tanzania	14.5	14.5	155	133	17
Gorilla	*Gorilla beringei*	Hominidae	Rwanda	9.5	15.5	151	151	19

For more detailed information on each study see refs. 11 and 12.

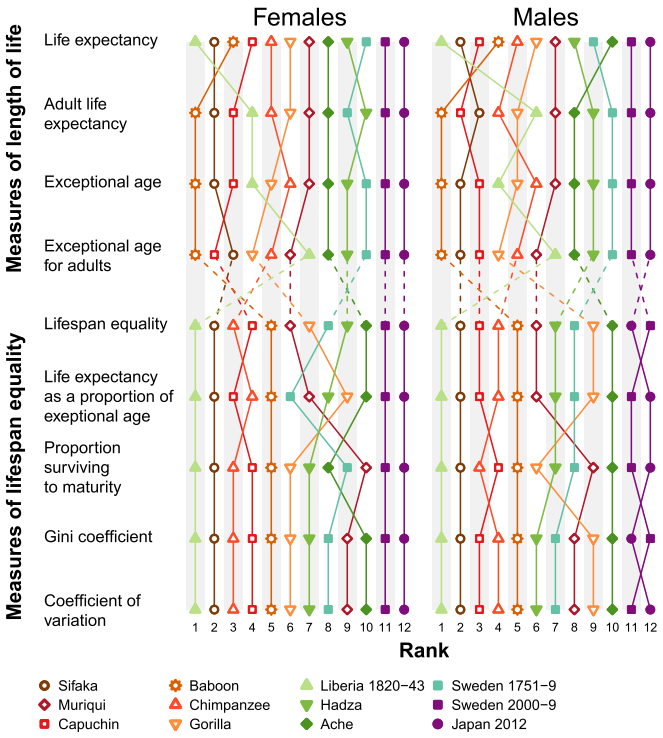

Fig. 2. Ranking of four measures of length of life and five measures of variation in lifespan, for females and males in the 12 focal populations. The rank ordering of the populations for each measure is shown in increasing order (lowest to the left, highest to the right).

a continuum from inequality to equality in lifespans, at least for primates (Figs. 2 and 3 and Table 2).

Relationship of Life Expectancy to Lifespan Equality

All our measures of the length of life (pace) show strong correlations with our measures of lifespan variation (shape); as lifespan increases, the relative variation in lifespan decreases (Fig. 2 and 3 and Table 2). Thus, the fast/slow and inequality/equality continua combine, for primates, into a single lifespan continuum. Notably, other taxa can show different patterns. For example, environmental and genetic manipulations can substantially alter the life expectancy of the nematode worm *Caenorhabditis elegans*, but the shape of the distribution of lifespans remains unaffected. These interventions rescale time to produce an extension or contraction of survival patterns, but when time is standardized, the shape of the distributions remains the same (22). In addition, although studies of lifespans from birth of animals in the wild are unusual, we found serviceable data for 15 species of wild nonhuman mammals. For these mammals the correlation between life expectancy and lifespan equality is not significant (Table S3). Similarly, 46 diverse species across the tree of life show no correlation between a measure of the length of life and a measure of relative variation in lifespans (23). In contrast, Baudisch et al. (24) reported a weakly positive but nonlinear relationship between their measures of the length of life and variation in lifespan in plants. The relationship between measures of pace and shape is not trivial and awaits further exploration.

To more deeply examine the relationship between life expectancy and lifespan equality, we supplemented data on our 6 human populations with information from 16 additional human populations (Table S4). We chose these additional populations based on the length of the time series and the quality of the available data, but we have confirmed that including data from additional populations does not significantly alter our findings. Examining pace–shape space by plotting life expectancy against lifespan equality reveals regularities across primates and over human experience (Fig. 4*A*).

For humans the linear relationship in Fig. 4*A* holds for both males and females, for populations in the 21st century and historically, for vastly different levels of life expectancy and vastly different societies. Consider the difference between life expectancies in two different populations and the corresponding difference between lifespan equalities. The regression line (Fig. 4*A*) implies that the first difference is about 28 times the second difference, regardless of whether the comparison is between (*i*) males vs. females in Russia in 2013, (*ii*) Swedish females in 1950–1959 vs. 1751–1759, (*iii*) Japanese females in 2013 vs. Liberian males in 1820–1843, or (*iv*) US vs. Nigerian males in 2013.

For industrialized human societies it is known that increases in life expectancy tend to be associated with greater lifespan equality: This is sometimes referred to as the compression of mortality or the rectangularization of survival curves (1, 2, 25). Here we demonstrate that lifespan equality tightly tracks life expectancy (Fig. 4 *A* and *B*) not just for long-lived industrialized populations but across the full range of human experience (Fig. 4 *A*–*C*) and for both males and females. In addition, we demonstrate that human and nonhuman primate populations fall into two separate lines (respectively gray and yellow in Fig. 4*A*) and that the primate and human lines intersect with preindustrial humans.

Fig. 4*B*, which summarizes more than 8,000 human life tables from a reliable database (19), shows, for various levels of life expectancy, the low variation in lifespan equality at all these various levels. The relationship is approximately linear. In the future, however, this trend may change to a logarithmic pattern. As survival improvements for infants, children, and younger adults result in an increasingly exponential rise in mortality with age, we observe a convergence of the trend with the blue curve

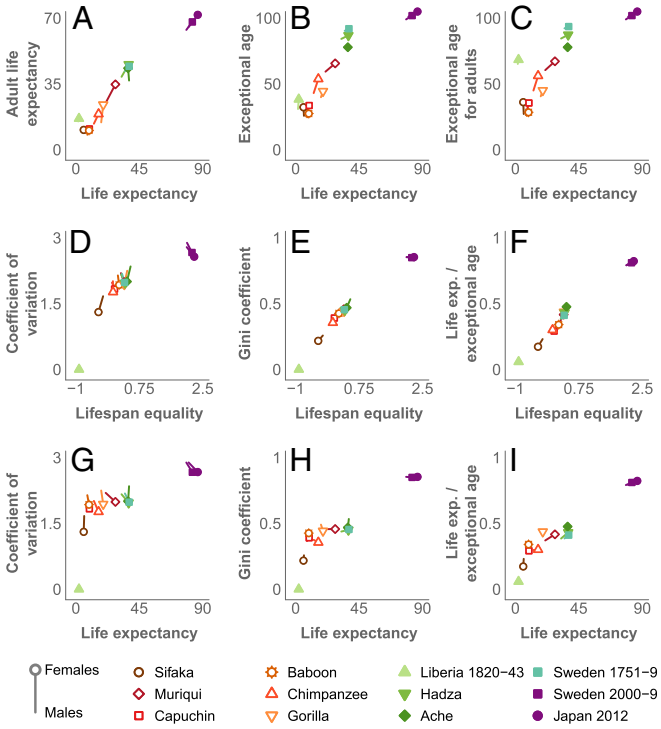

Fig. 3. Scatterplots showing relationships among selected measures of the length of life and lifespan equality for the 12 datasets analyzed. *A*–*C* show scatterplots between measures of length of life, *D*–*F* show comparisons between measures of lifespan equality, and *G*–*I* show scatterplots between length of life and measures of lifespan equality. For display purposes, the values of the Gini coefficient and the coefficient of variation were transformed by subtracting each population's value from the maximum in the dataset.

Table 2. Spearman's (open cells) and Pearson's (shaded cells) correlation coefficients between the measures of length of life and of lifespan equality for females and males of the 12 main populations

Measure	e_0	e_α	Ω_0	Ω_α	ε_0	l_α	e_0/Ω_0	g_0	cv_0
Females									
e_0	1.00	0.94	0.94	0.83	0.94	0.92	0.87	−0.92	−0.92
e_α	0.97	1.00	0.99	0.94	0.87	0.83	0.82	−0.83	−0.83
Ω_0	0.91	0.97	1.00	0.95	0.83	0.83	0.77	−0.82	−0.82
Ω_α	0.84	0.93	0.96	1.00	0.73	0.70	0.64	−0.70	−0.70
ε_0	0.96	0.87	0.77	0.65	1.00	0.91	0.96	−0.95	−0.95
l_α	0.90	0.83	0.77	0.59	0.96	1.00	0.88	−0.98	−0.98
e_0/Ω_0	0.95	0.89	0.81	0.68	0.99	0.98	1.00	−0.93	−0.93
g_0	−0.91	−0.83	−0.75	−0.59	−0.98	−0.99	−0.98	1.00	1.00
cv_0	−0.74	−0.65	−0.63	−0.39	−0.84	−0.95	−0.87	0.93	1.00
Males									
e_0	1.00	0.85	0.91	0.80	0.94	0.96	0.95	−0.92	−0.93
e_α	0.97	1.00	0.97	0.98	0.74	0.78	0.75	−0.71	−0.71
Ω_0	0.90	0.96	1.00	0.96	0.79	0.82	0.80	−0.76	−0.76
Ω_α	0.83	0.93	0.95	1.00	0.68	0.71	0.69	−0.63	−0.64
ε_0	0.95	0.85	0.75	0.61	1.00	0.92	0.99	−0.98	−0.97
l_α	0.91	0.84	0.82	0.64	0.95	1.00	0.93	−0.94	−0.95
e_0/Ω_0	0.94	0.85	0.78	0.63	0.99	0.97	1.00	−0.97	−0.98
g_0	−0.90	−0.8	−0.74	−0.56	−0.98	−0.98	−0.99	1.00	0.99
cv_0	−0.70	−0.58	−0.61	−0.34	−0.83	−0.90	−0.85	0.92	1.00

The row and column heads correspond to the following: e_0, life expectancy; e_α, adult life expectancy; Ω_0, exceptional age; Ω_α, exceptional age for adults; ε_0, lifespan equality; g_0, Gini coefficient; cv_0, coefficient of variation; l_α, proportion surviving to maturity; e_0/Ω_0, life expectancy as a proportion of exceptional age (see Box 1 and *Materials and Methods* for a full description of the measures).

(Fig. 4*B*), which marks the theoretical pace–shape relationship for an exponentially rising adult mortality trajectory (see Box 1 for further discussion).

In crises when humans suffer low levels of life expectancy similar to that of nonhuman primates, variation in lifespans among humans is comparatively greater than the variation among nonhuman primates at the same level of life expectancy. Even under extreme conditions in which most humans die very young, life tables include some humans at ages above 70 y, an age never approached by any nonhuman primate (Fig. 1). Hence human lifespan equality at low life expectancies is lower than in nonhuman primate species. Consider, for example, female baboons compared with women in the Ukraine in 1933, two populations with roughly equal life expectancies (9.34 y and 10.85 y, respectively) but very different values of lifespan equality. For the baboons, the maximum observed lifespan was just under 28 y. In the life table for the Ukrainian women, in contrast, 1% would survive past age 66 y.

Consistent with previous research (26–28), Fig. 4 *A* and *B* does not indicate that humans are approaching a looming limit to life expectancy. As noted above, it is possible that further increases in lifespan equality may be more difficult to achieve, in which case increases in life expectancy would largely come about by shifting the hump of deaths at older ages (Fig. 1) to even older ages, rather than by reducing the spread of this hump. In this case, lifespan equality would increase with the log of life expectancy (29). The postponement of old-age mortality has been ongoing in long-lived populations for more than half a century and may continue (28–30).

We analyzed how exceptionally high mortality and rapid changes in conditions would affect the relationship between pace and shape, using three short-term crisis populations when mortality sharply rose and then sharply declined from year to year: famine and a smallpox epidemic in Sweden (19) in 1773, a measles epidemic in Iceland (19) in 1882, and famine produced by forced efforts to collectivize farming in the Ukraine (31) in 1932–1934. Both life expectancy and lifespan equality fell and rose simultaneously and proportionally for both males and females (Fig. 4*C*) and did not diverge from the overall human line. This and other analyses of changes in life expectancy and lifespan equality over time (not reported here) suggest that the pace of life and the shape of the distribution of lifespans are so tightly bound together that they determine each other in a regular fashion that is not broken by exceptional circumstances. This result may spur innovative research on age patterns of mortality.

The yellow line in Fig. 4*A* was fitted to the data for our six nonhuman primate species plus a single point for humans that is a simple average of the points for six populations (the three hunter-gatherer datasets, Swedish populations in 1751–1759 and 1800–1809, and English parishes over the period 1600–1725) (*Materials and Methods*). These preindustrial human populations lie at the endpoint of the primate continuum and seem to describe a baseline human experience that prevailed until the industrial revolution.

Sex Differences in Lifespan

Among most of our 12 focal populations, females have both an absolute and a relative advantage at birth in life expectancy and lifespan equality. None of the sex differences within populations are statistically significant except for the 18th-century Swedish and the 21st-century populations, which show female advantages (Fig. 5). However, pooled mean and median values are significantly larger than 0 (one-sided *t*-test *P* values <0.001, all four panels of Fig. 5). Furthermore, the larger landscape shown in Fig. 4*A* illustrates that males are generally disadvantaged relative to females in both life expectancy and lifespan equality, across the primate order and at all levels of human life expectancy. This suggests that the general male disadvantage may be an evolutionarily conserved trait among primates (see refs. 32 and 33 for evolutionary hypotheses about the male disadvantage). For species and populations with shorter life expectancies, this male disadvantage tends to be small. The populations in which males have substantially lower life expectancy than females are generally populations in which a greater proportion of males die relatively young (Fig. 1). This lowers lifespan equality as well as life expectancy.

Although industrial humans are astoundingly different from nonindustrial humans and from nonhuman primates in life expectancy and lifespan equality, they are similar to other primate and human populations in the sex difference in life expectancy and lifespan equality (Fig. 5). The relative difference in life expectancy between men and women in industrial societies falls in the middle of the general primate distribution, although the relative difference in lifespan equality is greater than for any other primate species or human population (Fig. 5). Indeed, against the general trend toward more equal lifespans (Fig. 4), the absolute disparity in lifespans between human males and females has tended to widen as life expectancy has increased—although relative disparities have remained more constant. This finding may lead to deeper understanding of the male disadvantage in life expectancy.

Outlook

The conquest of early death through collective human efforts to avert mortality from disease and accidents has yielded lifespans that are both longer and more equal in modern industrial humans than at any other time or in any other species in the primate order (26, 27, 34). Indeed, 21st-century high-income countries occupy different positions in pace–shape space than our recent ancestors, having benefitted from dramatic increases in both life expectancy and lifespan equality. Millions of years of evolution, which molded the lifespan continuum of the nonhuman primates and nonindustrial humans, were followed by an astonishingly short spurt of recent human history, from the mid-19th century until today, during which social, economic, and public health advances allowed modern industrial humans to distance themselves farther from nonindustrial humans than those humans were from other primates.

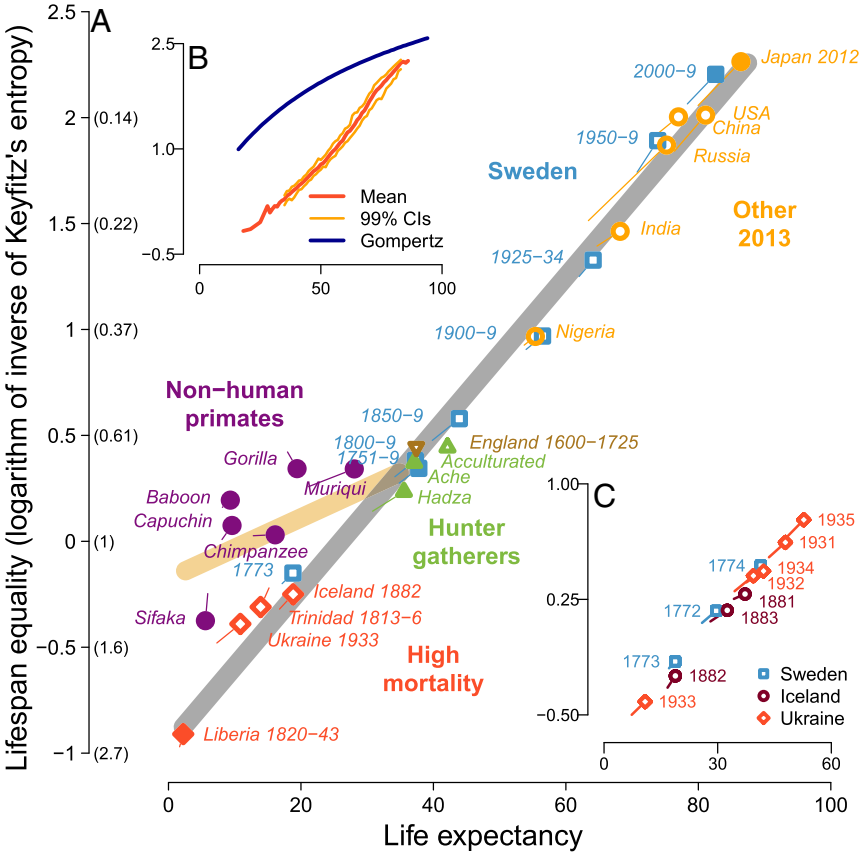

Fig. 4. The continuum of lifespan equality and life expectancy in primates. In *A*–*C*, the *y* axis shows our measure of lifespan equality, the log of the inverse of Keyfitz's entropy; corresponding values of Keyfitz's entropy are given in parentheses in *A*. (*A*) The evolutionary-historical continuum in lifespan equality and life expectancy for the 12 focal populations (Fig. 1) and 16 additional human populations (Table S4). The equation for the gray regression line is $\hat{e}_{0i} = -0.96 + 0.037\, e_{0i}$ (slope: $t = 41.45$, $P < 0.0001$, df = 20), and for the yellow regression line $\hat{e}_{0i} = -0.18 + 0.014\, e_{0i}$ (slope: $t = 3.34$, $P = 0.02$, df = 7), where $\hat{e}_{0i}$ denotes the estimated lifespan equality for the *i*th population and e_{0i} life expectancy. We also estimated a version of the yellow regression line using only hunter-gatherer data for humans: This line is $\hat{e}_{0i} = -0.17 + 0.0135\, e_{0i}$ (slope: $t = 3.17$, $P = 0.02$, df = 7). (*B*) The continuum for 8,198 human life tables. The blue curved line describes the relationship between lifespan equality and life expectancy if mortality follows Gompertz's law, i.e., if the risk of death rises exponentially, increasing 14%/y. Because of the paucity of observations, the 99% confidence intervals (CIs) are not shown for life expectancies below 35 y or over 85 y. (*C*) The continuum for three short-term crisis populations when mortality sharply rose and then sharply declined from year to year. In *A* and *C*, data for female–male pairs from each population are indicated by a point with a "tail"; the point represents female values, with male values at the end of the tail.

The extraordinary sociality of humans may both contribute to and be enhanced by the parallel rise of life expectancy and lifespan equality. A plausible hypothesis to be further explored is that highly social societies with prolonged, overlapping lifetimes and a substantial subpopulation with many years of accrued knowledge may be engines for reducing early deaths, propelling the increase of both life expectancy and lifespan equality. Not all individuals in these societies, however, benefit equally from these mutually reinforcing processes; considerable inequality in lifespans still exists in industrial human populations, in part because of disparities among socio-economic groups (35–42).

Inequality is generally more pronounced among men than among women. Further, our data show that lifespan equality for men lags behind that for women over historical time and during mortality crises. This male–female difference raises questions about the nature and extent of sex differences in how individuals survive hardship and illness and respond to socially mediated resources, opportunities, and risks, questions that remain largely unanswered (6, 7, 41, 42).

The emergence of longevous populations in which most individuals experience long lives is an extraordinary success of modern civilization. Describing the pace–shape space of life expectancy and lifespan equality enabled us to reveal the link between these two central components of the emergence of long-lived human populations. Why their relationship is roughly linear across primates and extraordinarily tight over human experience remains to be understood. The greater scatter around the nonhuman primate regression may be partially due to small sample sizes; accumulating data from additional natural populations of these and other primate species has the potential to shed considerable light on the relationship between pace and shape.

For humans, a positive association of life expectancy and lifespan equality is not surprising (1, 2). When life expectancy is low, some individuals nonetheless survive to old age, resulting in low lifespan equality. Increases in life expectancy are largely due to saving lives at ages younger than life expectancy, leading to an increase in lifespan equality (2). As life expectancy rises, the exceptional age that only 1% of newborns reach also rises but not

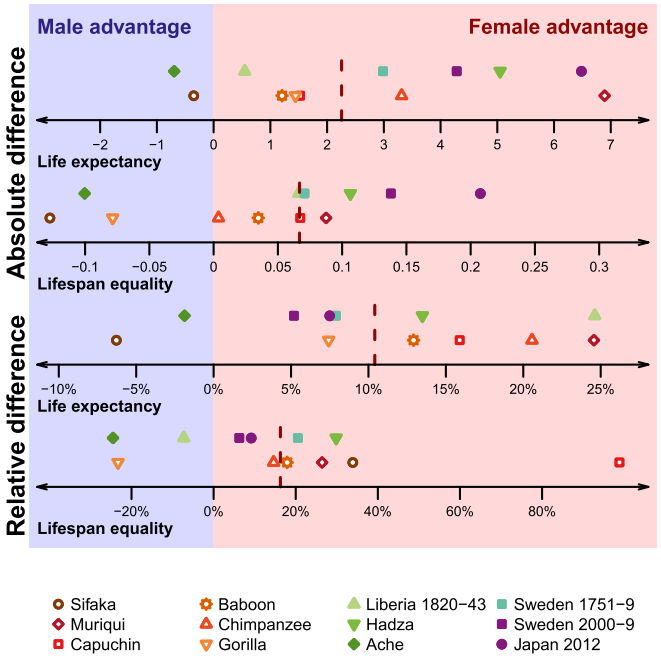

Fig. 5. Absolute and relative male–female differences in life expectancy and lifespan equality. Absolute differences between the male and female values are shown in the *Top* two panels; relative differences are shown in the *Bottom* two panels, expressed as the percentage of difference of males from females. Dark red dashed lines represent the median of each set of values; all medians lie in the direction of a female advantage.

proportionally (at least up until now). For instance, life expectancy and exceptional age for women were 2.2 y and 59 y for the Liberian population, 38 y and 91 y for Sweden in 1851–1859, and 87 y and 104 y for Japan in 2013. The narrowing of the ratio of exceptional age to life expectancy, from 27 to 2.4–1.2 for these three populations, increases lifespan equality. This trend does not imply that life expectancy is approaching a limit, although perhaps it is (25, 27–30).

The linearity of the relationship for humans between life expectancy and lifespan equality may prove useful but is not the central finding of our analysis. Use of measures based on the Gini coefficient or the coefficient of variation would produce other curves (Fig. 3), and moreover the curves in Fig. 4, especially Fig. 4*B*, are linear only to a first approximation. More important is that the environmental trend for humans is distinct from the evolutionary trend for primates, which has never been described before (Fig. 4*A*), and that the trend we identify for humans is not what would be predicted if death rates rose exponentially with age (Fig. 4*B*).

We find that the relationship between life expectancy and lifespan equality is, for both males and females, strong over primate evolution and extraordinarily strong across the range of human experience. We hypothesize that for humans this link is governed by fundamental features of human biology, including our exceptional sociality. Our results illustrate the power of biodemography, a nascent, transformational discipline that combines concepts, methods, questions, and theories from demography (43, 44) with related ideas from public health and from population biology and its sister disciplines of evolutionary biology, ecology, and life-history analysis, adding hybrid vigor to the Aristotelian and Darwinian roots of biology (27, 34, 45–51). This analytical strategy will yield further insights when applied to other clades across the tree of life. In particular, application of the pace–shape framework (3) to other species, as well as topics other than age at death (e.g., age at childbearing, marriage, or dementia), may lead to new results.

Materials and Methods

Data and Analyses for Human Populations. The data for the hunter-gatherer populations were obtained from published data on two populations, the Hadza and Ache (15, 16) (see Table 3 for summary information). Life tables for preindustrial 18th-century Sweden (1751–1759), modern Sweden (2000–2009), and modern Japan (2012) were drawn from the "Human Mortality Database" (HMD) (19). For these three datasets we extracted death counts by age (0–109 y), calendar year, and sex and corresponding exposure (Table 3). An additional 15 life tables for females and 15 life tables for males were obtained for Fig. 4*A* from the HMD for Sweden in different periods, Ukraine (1933), and Iceland (1882); from the "World Health Organization" (WHO) (54) for Nigeria, India, Russia, China, and the United States all for the year 2013; and from published sources for Liberian migrants (1820–1843) (17, 18),

Box 1. Demographic distributions and measures

Researchers who study survival and longevity construct life tables to reveal the implications of mortality regimes with age-specific risks of death fixed at prevailing levels. All of the measures used in this article are calculated from a life table and hence capture the intrinsic implications of a pattern of death rates. The measures do not pertain to a cohort of individuals aging together over time or to a population with an age structure shaped by previous mortality, fertility, and migration.

In life tables the distribution (probability density function) of ages at death in a population, i.e., the distribution of lifespans, denoted by $d(x)$ where x is age, is a fundamental function of the most profound interest (Fig. 1). Although populations are finite, most populations studied by demographers are large enough that $d(x)$ can be treated as continuous, permitting the elegant analysis of calculus. When populations are small, the data can be smoothed to produce a continuous $d(x)$.

The cumulative value of $d(x)$ after age a gives the proportion surviving (still living) at age a, $l(a) = \int_a^\infty d(x)dx$, because death comes to all. Note $l(0) = 1$. The ratio $d(x)/l(x)$ equals $\mu(x)$, the force of mortality, i.e., hazard of death, at age x.

Life expectancy, the average age at death, is given by $e_0 = \int_0^\infty x\, d(x)dx$ or, equivalently, by $e_0 = \int_0^\infty l(x)dx$. Remaining life expectancy at age a is $e_a = \int_a^\infty l(x)dx/l(a)$.

The shape of the distribution of lifespans can be measured in various ways, including the coefficient of variation, the Gini coefficient, and Keyfitz's entropy (2, 3, 5) (*Materials and Methods*). The Keyfitz measure is related to but not the same as the entropy used in physics and information science. Keyfitz's entropy is given by the ratio $e^\dagger/e_0$ (Fig. 1), where $e^\dagger$ measures life expectancy lost due to death: $e^\dagger = \int_0^\infty e_x d(x)dx$. Keyfitz's entropy is an indicator of lifespan inequality; its inverse is an indicator of lifespan equality as is the log of the inverse, the measure we used. On the vertical axis of Fig. 4*A* values of Keyfitz's entropy are given in parentheses. The values in parentheses above 1 imply that remaining life expectancy is higher, on average, after birth than at birth. This can occur when infant death rates are much higher than death rates at later ages. On the other hand, a value below 1 indicates that most people die at ages when remaining life expectancy is short. A value of 0.22, for example, indicates that on average when an individual dies, remaining life expectancy at the age of death is only 22% of life expectancy at birth.

Gompertz hypothesized that the force of mortality increased exponentially with age (52). This has not been true for any human population because infant, childhood, and early adult mortalities are substantial (53). In populations with long life expectancy, however, the Gompertz ideal is being approached. The blue curve in Fig. 4*B* describes the relationship between life expectancy and lifespan equality if the Gompertz curve holds with a relative rate of increase of 0.14/y, a value suggested by theoretical considerations (27). If life expectancy is high enough, then lifespan equality increases with the log of life expectancy (29).

In addition to life expectancy, e_0, and lifespan equality, ε_0, we extended our analysis to other relevant measures of the pace and shape of life. We denote age at maturity by α, so e_α is the expected length of adult life. Exceptional age, Ω_0, the age that only 5% of newborns reach, is defined by $l(\Omega_0) = 0.05$. Similarly, the age that 5% of adults attain is defined by $l(\Omega_0)/l(\alpha) = 0.05$.

Variation in the length of life can be assessed by the coefficient of variation (CV), i.e., the ratio of the SD of lifespans to the average lifespan. This measure of relative dispersion, often used by statisticians, is given by

$$\mathrm{CV} = \sqrt{\int_0^\infty (x - e_0)^2 d(x)dx}/e_0.$$

Variation in the length of life can also be measured by the Gini coefficient, a measure used by economists to study income inequality. It can be calculated as half of the average of the absolute differences between the lifespans of all pairs of individuals in a population—relative to average lifespan. Its formula can be written as $1 - \int_0^\infty l(x)^2 dx$, an expression that clearly indicates that it is a measure of the rectangularity of the survival curve $l(x)$.

Two additional simple measures of variation in lifespans are the proportion of newborns that reach maturity, $l(\alpha)$, and the ratio e_0/Ω_0 (see Tables S1 and S2 for resulting values).

Trinidad slaves (1813–1816) (55), and England (1600–1725) (56). Additionally, we obtained Siler mortality parameters estimated by ref. 57 for acculturated hunter-gatherers for both sexes combined. For Fig. 4*B*, we obtained 8,198 yearly period life tables from the HMD for 44 countries.

For the six main human populations we carried out a bootstrap analysis to estimate all our pace–shape measures. For most life tables except Liberia, we assume that the observed number of deaths was the outcome of a random Poisson process in a population with given exposures $N(x)$ and the given age-specific death rate, $\mu(x)$, as the "true" signal. For each jth bootstrap step, we randomly drew a new set of number of deaths for age x, $D_j(x)$, from a Poisson distribution with parameter $\lambda_x = \mu(x)\ N(x)$. From the $D_j(x)$s we estimated the resulting life table, using standard methods (43) and the subsequent pace and shape measures. We ran 20,000 bootstrap steps, which allowed us to calculate mean, SEs, and confidence intervals for each measure. In the case of Liberia, we assumed that the observed number of deaths was the outcome of a random binomial process with parameters $q(x)$ for the probability of death and the number of individuals entering the interval $[x, x + \Delta x]$, namely $P(x)$. We then drew $D_j(x)$ values from a binomial distribution with parameters $q(x)$ and $P(x)$. The next steps were equivalent to those for the Poisson bootstrap.

The values of life expectancy and lifespan equality plotted for other populations in Fig. 4 *A* and *B* were calculated from data from various sources, as indicated in Table S4. In some cases data were available for 5-y age categories: We estimated values for a single year of age by linear interpolation. When life tables were available for single years of time but we needed tables for multiyear periods of time, we then took simple averages over the period of the single-year values of life expectancy and lifespan equality. We applied these same methods to all other life tables in Fig. 4, except for the acculturated hunter-gatherers for which we used the estimated Siler mortality parameters provided by Gurven and Kaplan (57).

Smoothing of Life-Table Data for Fig. 1. To display the densities in Fig. 1 we smoothed the death rates for the hunter-gatherer populations using *P*-splines, because of small sample sizes in these populations, following the proposal of Eilers and Marx (58). We used the implementation by Camarda (59, 60) in R, which has been tailored for smoothing mortality in a Poisson framework. We also smoothed the data for historic Sweden (1751–1759). The reason was not insufficient data, as was the case for the hunter-gatherer population: Our dataset for historic Sweden included ∼8 million person years for each sex when pooling data across years (Table 3). Instead, the data for Sweden from that period suffer from strong age heaping (19, 61). We suppressed those artificial fluctuations over age by having a strong penalty term λ for the *P*-spline smoothing. Death rates at ages below 80 y for contemporary Sweden (2000–2009) and Japan (2012) were not modified or smoothed in any way. Mortality at ages 80 y and above for historic (1751–1799) and contemporary (2000–2009) Sweden as well as for the population of contemporary Japan (2012) was estimated using a logistic mortality model given by

$$\overline{\mu}(x) = \frac{ae^{bx}}{1 + \frac{a\gamma}{b}(e^{bx} - 1)}, \quad [1]$$

which expresses the population hazard $\mu(x)$ as a mixture of Gompertz-distributed hazards with Gamma-distributed "frailty" among individuals (62). We used the same parametric model to estimate mortality for historic Sweden, contemporary Sweden, and Japan at ages 80 y and higher.

We estimated the parameters in a standard Poisson maximum-likelihood framework, given by

$$\ln \mathcal{L}(\alpha, \beta, \gamma | D(\mathbf{x}) N(\mathbf{x})) = \sum_{x=80}^{\omega} D(x) \ln \overline{\mu}(x) - N(x)\overline{\mu}(x), \quad [2]$$

where $D(x)$ is the number of people dying at age x and corresponding exposure times $N(x)$; and $\mu(x)$ refers again to the population-level hazard of Eq. **1**.

We then estimated life tables and life expectancy, using standard methods (43). We obtained the mean survival time at age x of those who die at age x, typically denoted as $a(x)$, from the HMD for contemporary Japan as well as for historic and contemporary Sweden. Based on life table information for the number of survivors at age x, $l(x)$, and the number of person years lived $L(x)$ available for the Hadza, we used values of $a(0) = 0.3$, $a(1) = 0.4$, and $a(x) = 0.5$ for $x > 1$ for all hunter-gatherer populations.

Table 3. Descriptive statistics of human populations of hunter-gatherers (Ache and Hadza) and populations from Liberia, Sweden, and Japan

Population	Sex	Person years	Deaths
Ache	Women	6,738	151
	Men	9,368	202
	Total	16,106	353
Hadza	Women	6,218	182
	Men	6,100	227
	Total	12,318	409
Liberia, 1820–1843	Women	1,973	1,135
	Men	2,318	967
	Total	4,291	2,195
Sweden, 1751–1759	Women	8,736,291	232,161
	Men	7,808,644	225,428
	Total	16,544,934	457,589
Sweden, 2000–2009	Women	45,582,428	475,035
	Men	44,832,800	446,825
	Total	90,415,228	921,860
Japan, 2012	Women	64,657,932	600,833
	Men	61,362,195	655,526
	Total	126,020,126	1,256,359

Person years are a combined measure of the number of individuals and the number of years they contributed to the study.

Data for Nonhuman Primates. We obtained data for six species of nonhuman primates from the Primate Life History Database (PLHD) (11), which includes longitudinal life-history data for known individuals in six study populations (Table 1). All populations in the PLHD are living in the wild and, with few exceptions, no provisioning or interventions have occurred in any of these populations (11). For all of these primate species one or both sexes undergo natal dispersal (first dispersal after birth), whereas four (baboons, gorillas, sifakas, and capuchin monkeys) have secondary or higher-order dispersals (Table S5).

For each of the six primate populations, the study population was defined as the set of social groups in which individuals were continuously monitored for life-history events. With one exception (muriquis), all study populations were embedded in larger continuous populations that were not isolated from the social groups being studied; consequently, individuals could immigrate into and emigrate from the study population, resulting in a situation in which some individuals were not observed throughout their entire lives. In the case of the muriquis, research expanded to encompass all four social groups in the entire isolated study population in the early 2000s, about 20 y into the research project. Thus, for muriquis subsequent to 2003 individuals could leave the study population but there was no immigration into the study population. All told, the database included nine different types of individual records in two broad categories (Fig. S2): (*i*) natal individuals, i.e., individuals that were live born in the study population, and (*ii*) immigrants, i.e., individuals born in social groups that were not part of the study population before their appearance in a study group, who emigrated from their natal social group and immigrated into a study group. For all six studies there were a considerable number of individuals with unknown fate, for both natals and immigrants, because an individual that belongs to the dispersing sex, has reached dispersal age, and disappears could have either died or attempted to disperse into a social group outside the study population.

Two further aspects of the data required estimation procedures. First, most immigrants had estimated birthdates (i.e., their ages were estimated at immigration). Individuals also had estimated birthdates if they were present in the study population at the time monitoring of the study population first began and they were first individually identified. Second, in most populations, some infants died before their sex was ascertained, resulting in deaths of infants with unknown sex.

Because of these sources of uncertainty, we constructed a Bayesian model to estimate mortality in these populations. Our model included estimation procedures for age and sex in cases where these were not known exactly and incorporated the probability of emigration for both natals and immigrants.

Bayesian Model for Nonhuman Primate Data with Sex-Specific Dispersal. We used an extension of the Bayesian approach proposed by Barthold et al. (13) to model age- and sex-specific mortality for species where one or both sexes undergo natal dispersal. The model builds upon the Bayesian survival trajectory analysis framework (63, 64) to model sex-specific mortality. We extended the model to include species for which one or both sexes undergo higher-order

dispersal as well as the estimation of unknown times of birth (for a full model description see refs. 13 and 14).

This approach allowed us to estimate the essential latent states of sex, age, and dispersal state and hence the parameters for mortality and out-migration from each study population (hereafter termed out-migration). We defined the random variables X for ages at death, Y for ages at natal out-migration, and Z for ages at immigrant out-migration. We defined a dispersal state D that assigns 1 if an individual i out-migrates in its last detection age, $x_i^L = t_i^L - b_i$, and 0 if otherwise. We treated D as a latent variable for all individuals with unknown fate. We also defined a variable S that assigns 1 if an individual is female and 0 otherwise.

The mortality function or hazard rate is

$$\mu(x) = \lim_{\Delta x \to 0} \frac{\Pr(x < X < x + \Delta x | X > x)}{\Delta x}.$$

We assumed that the mortality function in all of the primate species analyzed was well described by the Siler hazards rate (65) given by

$$\mu(x|\boldsymbol{\theta}) = \exp[\alpha_0 - \alpha_1 x] + \kappa + \exp[\beta_0 + \beta_1 x], \quad x \geq 0, \qquad [3]$$

where $\boldsymbol{\theta}^\top = [\alpha_0, \alpha_1, \kappa, \beta_0, \beta_1]$ is a vector of mortality parameters to be estimated, with α_0, $\beta_0 \in (-\infty, \infty)$ and α_1, κ, $\beta_1 > 0$. From the hazard rate in Eq. **3** we define the survival function

$$\begin{aligned} l(x|\boldsymbol{\theta}) &= \Pr(X > x) = \exp\left[-\int_0^x \mu(t|\boldsymbol{\theta})dt\right] \\ &= \exp\left[\frac{e^{\alpha_0}}{\alpha_1}(e^{-\alpha_1 x} - 1) - \kappa x + \frac{e^{\beta_0}}{\beta_1}(1 - e^{\beta_1 x})\right], \end{aligned} \qquad [4a]$$

the probability density function (PDF) of ages at death

$$d(x|\boldsymbol{\theta}) = \mu(x|\boldsymbol{\theta}) l(x|\boldsymbol{\theta}), \quad x > 0, \qquad [4b]$$

and the cumulative distribution function (CDF) for ages at death given by $F(x|\boldsymbol{\theta}) = 1 - l(x|\boldsymbol{\theta})$.

For out-migration, we assumed that the age at natal out-migration was $Y \sim G_Y(y|\gamma)$ for ages $y > 0$, where $G_Y(y)$ is the Gamma distribution function with parameter vector $\gamma = [\gamma_1, \gamma_2]$. This distribution yields the PDF of ages at natal out-migration given by

$$g_Y(y|\gamma) = \begin{cases} \frac{\gamma_1^{\gamma_2}}{\Gamma(\gamma_2)}(y - y_d)^{\gamma_2 - 1} e^{-\gamma_1 (y - y_d)} & \text{if } y \geq y_d \\ 0 & \text{if } y < y_d, \end{cases} \qquad [5]$$

where y_d is the minimum age at natal dispersal and γ_1, $\gamma_2 > 0$.

For immigrants in species with higher-order dispersal we assumed that the age at immigrant out-migration was $Z \sim G_Z(z|\lambda)$ for ages $z > 0$, where $\lambda = [\lambda_1, \lambda_2]$ is the vector of parameters to be estimated. The PDF of ages at immigrant out-migration is then

$$g_Z(z|\lambda) = \begin{cases} \frac{\lambda_1^{\lambda_2}}{\Gamma(\lambda_2)}(z - z_d)^{\lambda_2 - 1} e^{-\lambda_1 (z - z_d)} & \text{if } z \geq z_d \\ 0 & \text{if } z < z_d, \end{cases} \qquad [6]$$

with λ_1, $\lambda_2 > 0$ and where z_d is the minimum age at higher-order dispersal. Here we assumed that $z_d = y_d$.

The full Bayesian model is given by

$$\begin{aligned} p(\mathbf{d}_u, \mathbf{s}_u, \mathbf{b}_u, \boldsymbol{\theta}, \gamma, \lambda | \mathbf{d}_k, \mathbf{s}_k, \mathbf{b}_k, \mathbf{t}^F, \mathbf{t}^L) \propto & \underbrace{p(\mathbf{d}_k, \mathbf{s}_k, \mathbf{b}_k, \mathbf{t}^F, \mathbf{t}^L | \mathbf{d}_u, \mathbf{s}_u, \mathbf{b}_u, \boldsymbol{\theta}, \gamma, \lambda)}_{\text{likelihood}} \\ & \times \underbrace{p(\mathbf{d}) p(\mathbf{s}) p(\mathbf{x})}_{\text{priors for states}} \\ & \times \underbrace{p(\boldsymbol{\theta}) p(\gamma) p(\lambda)}_{\text{priors for parameters}}, \end{aligned} \qquad [7]$$

where $\mathbf{d}$ is the vector of dispersal states (i.e., $d_i = 1$ if the individual out-migrated and 0 otherwise), $\mathbf{s}$ is the indicator vector for females ($s_i = 1$ if female and 0 if male), $\mathbf{b}$ is a vector of ages at birth, and $\mathbf{t}^F$ and $\mathbf{t}^L$ are the vectors of times at first and last detection, respectively, where $\mathbf{x}^F = \mathbf{t}^F - \mathbf{b}$, and $\mathbf{x}^L = \mathbf{t}^L - \mathbf{b}$. Each of these vectors has two subsets represented by the subscripts u for unknown and k for known.

To estimate the parameters and latent states we used a Markov chain Monte Carlo (MCMC) algorithm to fit the model in Eq. **7** that uses a Metropolis-within-Gibbs sampling framework (66, 67) (for details of the estimation, see refs. 13 and 14). In addition to the implementation in refs. 13 and 14, we extended the model to estimate unknown times of birth. The conditional posterior for unknown times of birth, b_i, is

$$p(b_i | d_i, x_i^L, x_i^F, \boldsymbol{\theta}, \gamma, \lambda) \propto p(d_i, x_i^L, x_i^F, \boldsymbol{\theta}, \gamma, \lambda | b_i) \; p\left(b_i | b_i^L, b_i^U\right), \qquad [8]$$

where the first term in Eq. **8** corresponds to the likelihood function and the second term is a prior for times of birth. These priors are either uniform or normally distributed, both with upper and lower bounds provided with the dataset (i.e., b^L and b^U).

Estimation of Prior Parameters. To estimate the prior parameters for the mortality and out-migration parameters, we used a combination of published data, expert information provided by the PLHD coauthors, and an agent-based model designed to simulate natal and immigrant out-migration. The model required the parameters for adult mortality provided in Bronikowski et al. (12). Because these were calculated only for adults, we fixed the prior parameters that control juvenile mortality in the first exponential term of the Siler model in Eq. **1** at $\alpha_0^* = -2$ and $\alpha_1^* = 0.3$. We then used nonlinear least-squares estimation to find the remaining three parameters of the Siler model, using as reference the adult age-specific mortality constructed with the parameters found in ref. 12. For each species we calculated the sum of squares as

$$Q\left(\boldsymbol{\theta}_p^* | \boldsymbol{\theta}_b\right) = \sum_{i \in \mathbf{v}} \left[\mu\left(x_i | \boldsymbol{\theta}_p^*\right) - \mu_g(x_i - x_m | \boldsymbol{\theta}_b)\right]^2, \qquad [9]$$

where $\boldsymbol{\theta}_p^*$ was the vector of prior mortality parameters to be estimated, $\mu(x|\boldsymbol{\theta}^*)$ was the Siler hazards rate constructed with the prior parameters, $\mu_g(x - x_m \mid \boldsymbol{\theta}_b) = a \exp[b\,(x - x_m)]$ with a, $b > 0$ was the Gompertz mortality function where $\boldsymbol{\theta}_b = [a, b]$ was the vector of parameters estimated in ref. 12, and $\mathbf{v}^\top = [x_1, x_2, \ldots, x_T]$ was a sequence of $T = 10$ equally distanced ages starting at the age at maturity $x_1 = x_m$ and with last age x_T, such that the Gompertz survival with parameters $\boldsymbol{\theta}_b$ was $S_g(x_T | \boldsymbol{\theta}_b) = 0.05$. We used the R built-in function nlm to find the prior parameters $\boldsymbol{\theta}_p$ that minimized the sum of squares in Eq. **9** (see Table S6 for mean values for prior parameters).

To estimate the priors for out-migration parameters γ and λ, we implemented an agent-based model. We used published information on dispersal behavior for each species as well as expert information provided by the PLHD researchers. Then, for each species we simulated a hypothetical population of dispersing individuals that could disperse between study groups, represented by set G, or to nonstudy groups, defined by set A, with universal set $S = \{G \cup A\}$ that represented all of the possible groups for each population. The number of groups in G and A varied among the six studies, and any movement between groups (either study or external groups) is considered to represent dispersal in the population.

To parameterize the density functions of ages at natal and higher-order dispersal we used information on minimum, maximum, and average ages at natal and higher-order dispersal provided in the literature and by the PLHD researchers. We calculated mean, $\bar{y}_1$ for natal, and $\bar{y}_2$ for higher-order dispersal and variances σ_1^2 for natal and σ_2^2 for higher-order dispersal and estimated the corresponding Gamma parameters as

$$\alpha_j = \frac{\bar{y}_j^2}{\sigma_j^2} \quad \text{and} \quad \beta_j = \frac{\bar{y}_j}{\sigma_j^2},$$

for $j = 1,2$, where α_j and β_j are the shape and rate parameters for the natal and higher-order dispersal (see Table S7 for resulting parameters).

We used an individual-based model to simulate mortality and dispersal, to find the prior parameters for the distribution function of ages at natal and immigrant out-migration. The step-by-step algorithm for first dispersal is as follows: (*i*) For every individual i simulate age at death (x_i) from a Siler mortality function with parameters $\boldsymbol{\theta}_p$; (*ii*) simulate ages at natal dispersal (y_i^1) by randomly sampling from a Gamma distribution with parameters $\{\alpha_1, \beta_1\}$; (*iii*) individuals where $x_i > y_i^1$ successfully dispersed, and otherwise they died before dispersing for the first time; (*iv*) all dispersers move with the same probability to any of the groups within the study population (G) or to one of the areas outside the study population (A); (*v*) those individuals that moved to set A have out-migrated and their age at out-migration y_i is stored, and those that moved to set G have remained in the population; (*vi*) in species with higher-order dispersal, those in set G disperse again at a further age (y_i^2) by randomly sampling from a Gamma distribution with parameters $\{\alpha_2, \beta_2\}$; (*vii*) individuals where $x_i > y_i^2$ can disperse to any group in G or A, and otherwise they died before dispersing again; and (*viii*) repeat steps *vi* and *vii* until all individuals are either dead at age x_i or have out-migrated at age y_i.

All individuals that had out-migrated were assigned the indicator $d_i = 1$ and those that died before migrating were assigned $d_i = 0$. We then took the results to construct the log-likelihood

$$\ln \mathcal{L}(\gamma_p|\mathbf{y},\mathbf{x}) = \sum_{d_i=1} \ln\left[g(y_i|\gamma_p)\right] + \sum_{d_i=0} \ln\left[1-G(x_i|\gamma_p)\right], \quad [10]$$

where γ_p is a vector of natal out-migration prior parameters to be estimated. These parameters were then used in the main model as uninformative priors (with large SEs) for natal out-migration in Eq. **7**.

We followed a similar procedure to estimate the prior parameters for secondary out-migration applied to immigrants in the main model. To do this, we used all individuals that had out-migrated from the previous results and assumed that they were moving into the study population. Here is the algorithm for secondary out-migration (which applies only in species that show secondary out-migration): (*i*) All immigrants are potential secondary dispersers; (*ii*) simulate age at dispersal (y_i^t) by randomly sampling from a gamma distribution with parameters $\{\alpha_2, \beta_2\}$; (*iii*) if $x_i > y_i^t$, allow the individual to move to any group in *G* or in *A* with same probability; (*iv*) all dispersers that moved to *A* have out-migrated and are assigned an age at dispersal y_i, and those that moved to set *G* have remained in the study population; and (*v*) repeat *ii* and *iii* with all individuals that moved to *G* until all either are dead at ages x_i or have out-migrated at ages y_i.

All individuals that had out-migrated were assigned the indicator $d_i = 1$ and those that died before migrating were assigned $d_i = 0$. We then took the results to construct the log-likelihood for ages at secondary out-migration

$$\ln \mathcal{L}(\lambda_p|\mathbf{y},\mathbf{x}) = \sum_{d_i=1} \ln\left[g(y_i|\lambda_p)\right] + \sum_{d_i=0} \ln\left[1-G(x_i|\lambda_p)\right], \quad [11]$$

where λ_p is the vector of immigrant out-migration prior parameters to be estimated. These parameters were then used in the main model as informative priors (with low SEs) for immigrant out-migration in Eq. **7**.

Regressions Between Life Expectancy and Lifespan Equality. In Fig. 4*A* we depict two regression lines between lifespan equality and life expectancy. The gray line corresponds to the regression over the 22 human populations. Because the data included eight time spans for Sweden, we performed the Durbin–Watson test (68) to determine the level of serial autocorrelation in the residuals. The test was not significant ($D > D_u$ with $D = 1.48$, upper critical value $D_u = 1.174$ for alpha level 0.01).

For the primate regression line (i.e., yellow line in Fig. 4*A*) we used all six nonhuman primate estimates and averaged the estimates for Sweden 1751–1759 and 1800–1809 and England 1600–1725, as well as the Ache, Hadza, and acculturated hunter-gatherer estimates. Thus, we had a single pair of values for each of the seven species, with the values for humans being averaged over six populations. We then implemented a weighted phylogenetic generalized least-squares regression model on the female points, with weights given by

$$w_i = \frac{1}{N_i}\sum_{j=1}^{N_i} n_j, \quad \text{for } i = 1, \ldots, 7,$$

where N_i is the total number of datasets for the data point *i*, and n_j is the sample size for the *j*th population. The phylogenetic component of this regression model was the variance–covariance (VCV) matrix, which we based on the phylogenetic relationships (and therefore statistical nonindependence) of the seven species. To account for phylogenetic signal we transformed this VCV matrix using Pagel's lambda (69), which we optimized using maximum likelihood. We obtained a consensus tree for the seven primates from the *10kTrees* website (70), but substituted *Brachyteles arachnoides* for *Brachyteles hypoxanthus* because phylogenetic data for the latter were not available.

The resulting coefficients of this phylogenetic generalized least-squares regression were $\hat{\varepsilon}_{0i} = -0.18 + 0.014\, e_{0i}$, where $\hat{\varepsilon}_{0i}$ denotes the estimated lifespan equality for the *i*th population and e_{0i} life expectancy (slope: $t = 3.34$, $P = 0.02$, df = 7), with an optimized value of Pagel's lambda of $\lambda = 0.861$ (i.e., strong phylogenetic signal).

Upper Limit for Density Curves in Fig. 1. As a general rule the ages to plot the probability density functions in Fig. 1 range from age 1 y to the age when $l_x = 0.01$; this is when 1% of the cohort is still alive. The only exceptions are the curves for the muriqui due to the large amount of censoring in the data and the resulting uncertainty in the curves. In addition, for the nonhuman primates, we shaded the polygons and used dashed lines after the maximum estimated age in our populations to highlight that after those ages the curves correspond to predicted values.

Data Preparation for Additional Mammal Species and Analysis. We obtained life tables for females of nine additional mammal species from seven taxonomic families and ranging in body size from the ∼50-g tundra vole (*Microtus oeconomus*) to the 800-kg gaur (*Bos gaurus*). These data were obtained from the DatLife database (www.demogr.mpg.de/en/laboratories/evolutionary_biodemography_1171/projects/datlife_the_demography_of_aging_across_the_tree_of_life_database_744.htm), and the ultimate sources are given in Table S3. For each life table we calculated life expectancy at birth (e_0) and lifespan equality (ε_0), using the equations given in Box 1, as for humans and other primates.

We then implemented a phylogenetic generalized least-squares regression model on the female points for the six primate species and the nine additional mammals. The phylogenetic component of this regression model was the VCV matrix, which we based on the phylogenetic relationships (and therefore statistical nonindependence) of the 15 species. To account for phylogenetic signal we transformed this VCV matrix using Pagel's lambda (69), which we optimized using maximum likelihood. We obtained a consensus tree for the 15 mammals from ref. 71 hosted at the *Evo10* website (https://www.evoio.org/wiki/File:Bininda-emonds_2007_mammals.nex). Because the phylogenetic data for *B. arachnoides* and *Papio cynocephalus* were not available, we substituted them for *B. hypoxanthus* and *Papio hamadryas*, respectively.

The resulting coefficients of this phylogenetic generalized least-squares regression were $\hat{\varepsilon}_{0i} = -0.2 + 0.018\, e_{0i}$,, where $\hat{\varepsilon}_{0i}$ denotes the estimated lifespan equality for the *i*th population and e_{0i} life expectancy (slope: $t = 1.99$, $P = 0.07$, df = 13), with an optimized value of Pagel's lambda of $\lambda = 0$ (i.e., no phylogenetic signal).

All statistical analyses were performed in the open-source free package R (72).

ACKNOWLEDGMENTS. We thank S. H. Preston for cogent suggestions. We thank M. Cords, A. van Raalte, and various researchers associated with the Max Planck Institute for Demographic Research and the Max-Planck Odense Center on the Biodemography of Aging, as well as the students in the 2014–2015 year of the European Doctoral School of Demography, for helpful comments. We thank M. Cords and W. F. Morris for assistance with designing the Primate Life Histories Database. The authors thank the multiple funding agencies, government bodies, and researchers that made possible the data collection behind the Primate Life Histories Database (see Acknowledgments at https://plhdb.org/ for more information). Our research was supported by the Max Planck Society, the Max Planck Institute for Demographic Research, the University of Southern Denmark, the National Evolutionary Synthesis Center, the National Center for Environmental Analysis and Synthesis, the Princeton Centers for the Demography of Aging and for Health and Well-Being, and the US National Institute on Aging (Grants P01AG031719 and R01AG034513).

1. Smits J, Monden C (2009) Length of life inequality around the globe. *Soc Sci Med* 68(6):1114–1123.
2. Vaupel JW, Zhang Z, van Raalte AA (2011) Life expectancy and disparity: An international comparison of life table data. *BMJ Open* 1(1):e000128.
3. Baudisch A (2011) The pace and shape of ageing. *Methods Ecol Evol* 2(4):375–382.
4. Wrycza T, Baudisch A (2014) The pace of aging: Intrinsic time scales in demography. *Demogr Res* 30:1571–1590.
5. Wrycza TF, Missov TI, Baudisch A (2015) Quantifying the shape of aging. *PLoS One* 10(3):e0119163.
6. Marmot MG (2004) *The Status Syndrome: How Social Standing Affects Our Health and Longevity* (Macmillan, London).
7. Holt-Lunstad J, Smith TB, Layton JB (2010) Social relationships and mortality risk: A meta-analytic review. *PLoS Med* 7(7):e1000316.
8. Castelló-Climent A, Doménech R (2008) Human capital inequality, life expectancy and economic growth. *Econ J* 118(528):653–677.
9. Pusey AE (2012) Magnitude and sources of variation in female reproductive performance. *The Evolution of Primate Societies*, eds Mitani JC, Call J, Kappeler PM, Palombit RA, Silk JB (Univ of Chicago Press, Chicago).
10. Silk JB (2007) Social components of fitness in primate groups. *Science* 317(5843):1347–1351.
11. Strier KB, et al. (2010) The Primate Life History Database: A unique shared ecological data resource. *Methods Ecol Evol* 1(2):199–211.
12. Bronikowski AM, et al. (2011) Aging in the natural world: Comparative data reveal similar mortality patterns across primates. *Science* 331(6022):1325–1328.
13. Barthold JA, Packer C, Loveridge AJ, Macdonald DW, Colchero F (2016) Dead or gone? Bayesian inference on mortality for the dispersing sex. *Ecol Evol* 6(14):4910–4923.
14. Barthold JA, Loveridge AJ, Macdonald DW, Packer C, Colchero F (2016) Bayesian estimates of male and female African lion mortality for future use in population management. *J Appl Ecol* 53(2):295–304.
15. Blurton Jones N (2016) *Demography and Evolutionary Ecology of Hadza Hunter-Gatherers* (Cambridge Univ Press, Cambridge, UK).
16. Hill KR, Hurtado AM (1996) *Aché Life History: The Ecology and Demography of a Foraging People* (Transaction Publishers, Piscataway, NJ).
17. McDaniel A (1992) Extreme mortality in nineteenth-century Africa: The case of Liberian immigrants. *Demography* 29(4):581–594.
18. McDaniel A, Preston SH (1994) Patterns of mortality by age and cause of death among nineteenth-century immigrants to Liberia. *Popul Stud* 48(1):99–115.

19. Human Mortality Database University of California, Berkeley (USA), and Max Planck Institute for Demographic Research (Germany). Available at www.mortality.org. Accessed February 1, 2016.
20. Jones OR, et al. (2008) Senescence rates are determined by ranking on the fast-slow life-history continuum. *Ecol Lett* 11(7):664–673.
21. Zhang Z, Vaupel J (2009) The age separating early deaths from late deaths. *Demogr Res* 20:721–730.
22. Stroustrup N, et al. (2016) The temporal scaling of Caenorhabditis elegans ageing. *Nature* 530(7588):103–107.
23. Jones OR, et al. (2014) Diversity of ageing across the tree of life. *Nature* 505(7482): 169–173.
24. Baudisch A, et al. (2013) The pace and shape of senescence in angiosperms. *J Ecol* 101(3):596–606.
25. Fries JF (1980) Aging, natural death, and the compression of morbidity. *N Engl J Med* 303(3):130–135.
26. Oeppen J, Vaupel JW (2002) Demography. Broken limits to life expectancy. *Science* 296(5570):1029–1031.
27. Vaupel JW (2010) Biodemography of human ageing. *Nature* 464(7288):536–542.
28. Rau R, Soroko E, Jasilionis D, Vaupel JW (2008) Continued reductions in mortality at advanced ages. *Popul Dev Rev* 34(4):747–768.
29. Vaupel JW (1986) How change in age-specific mortality affects life expectancy. *Popul Stud* 40(1):147–157.
30. Bongaarts J (2009) Trends in senescent life expectancy. *Popul Stud* 63(3):203–213.
31. Meslé F, Vallin J (2012) *Mortality and Causes of Death in 20th-Century Ukraine* (Springer Science & Business Media, Berlin).
32. Austad SN (2006) Why women live longer than men: Sex differences in longevity. *Gend Med* 3(2):79–92.
33. Clutton-Brock TH, Isvaran K (2007) Sex differences in ageing in natural populations of vertebrates. *Proc Biol Sci* 274(1629):3097–3104.
34. Burger O, Baudisch A, Vaupel JW (2012) Human mortality improvement in evolutionary context. *Proc Natl Acad Sci USA* 109(44):18210–18214.
35. van Raalte AA, et al. (2011) More variation in lifespan in lower educated groups: Evidence from 10 European countries. *Int J Epidemiol* 40(6):1703–1714.
36. van Raalte AA, Martikainen P, Myrskylä M (2014) Lifespan variation by occupational class: Compression or stagnation over time? *Demography* 51(1):73–95.
37. Gillespie DOS, Trotter MV, Tuljapurkar SD (2014) Divergence in age patterns of mortality change drives international divergence in lifespan inequality. *Demography* 51(3):1003–1017.
38. Shkolnikov VM, Andreev EM, Zhang Z, Oeppen J, Vaupel JW (2011) Losses of expected lifetime in the United States and other developed countries: Methods and empirical analyses. *Demography* 48(1):211–239.
39. Edwards RD, Tuljapurkar S (2005) Inequality in life spans and a new perspective on mortality convergence across industrialized countries. *Popul Dev Rev* 31(4): 645–674.
40. Tuljapurkar S, Edwards RD (2011) Variance in death and its implications for modeling and forecasting mortality. *Demogr Res* 24:497–526.
41. Cohen B, Preston SH, Crimmins EM, eds (2011) *Explaining Divergent Levels of Longevity in High-Income Countries* (Natl Acad Press, Washington, DC).
42. Cohen B, Preston SH, Crimmins EM, eds (2011) *International Differences in Mortality at Older Ages: Dimensions and Sources* (Natl Acad Press, Washington, DC).
43. Preston SH, Heuveline P, Guillot M (2001) *Demography. Measuring and Modeling Population Processes* (Blackwell, Oxford).
44. Wachter KW (2014) *Essential Demographic Methods* (Harvard Univ Press, Cambridge, MA).
45. Wachter KW, Finch CE (1997) *Between Zeus and the Salmon: The Biodemography of Longevity*, eds Wachter KW, Finch CE (Natl Acad Press, Washington, DC).
46. Carey JR, Judge DS (2001) Principles of biodemography with special reference to human longevity. *Population* 13(1):9–40.
47. Carey JR, Vaupel JW (2005) Biodemography. *Handbook of Population*, eds Poston DL, Micklin M (Springer, New York), pp 625–658.
48. Wachter KW (2008) Biodemography comes of age. *Demogr Res* 19(40):1501–1512.
49. Baudisch A, Vaupel JW (2012) Evolution. Getting to the root of aging. *Science* 338(6107):618–619.
50. Wachter KW, Steinsaltz D, Evans SN (2014) Evolutionary shaping of demographic schedules. *Proc Natl Acad Sci USA* 111(Suppl 3):10846–10853.
51. Grundy E, Murphy M (2015) Demography and public health. *Oxford Textbook on Public Health*, eds Detels R, Gulliford M, Karim QA, Tan CC (Oxford Univ Press, Oxford), 6th Ed, pp 718–735.
52. Gompertz B (1825) On the nature of the function expressive of the law of human mortality, and on a new mode of determining the value of life contingencies. *Philos Trans R Soc Lond* 115(0):513–583.
53. Vaupel J, Zhang Z (2010) Attrition in heterogeneous cohorts. *Demogr Res* 23:737–748.
54. WHO (2016) WHO Life Tables. Available at www.who.int/gho/mortality_burden_disease/life_tables/life_tables/en/ and apps.who.int/gho/data/node.main.692?lang=en. Accessed June 6, 2016.
55. John AM (2002) *The Plantation Slaves of Trinidad, 1783-1816* (Cambridge Univ Press, New York).
56. Wrigley EA, Davies RS, Oeppen J, Schofield RS (1997) *English Population History from Parish Reconstitutions* (Cambridge Univ Press, Cambridge, UK).
57. Gurven M, Kaplan H (2007) Longevity among hunter-gatherers: A cross-cultural examination. *Popul Dev Rev* 33(2):321–365.
58. Eilers PHC, Marx BD (1996) Flexible smoothing with B-splines and penalties. *Stat Sci* 11(2):89–121.
59. Camarda CG (2012) MortalitySmooth: An R package for smoothing Poisson counts with P-Splines. *J Stat Softw* 50(1):1–24.
60. Camarda CG (2009) Smoothing methods for the analysis of mortality development. PhD thesis (Universidad Carlos III de Madrid, Madrid).
61. Glei DA, Lundström H, Wilmoth JR (2007) *About Mortality Data for Sweden* (Human Mortality Database, Berkeley, CA).
62. Vaupel JW, Missov TI (2014) Unobserved population heterogeneity. *Demogr Res* 31: 659–686.
63. Colchero F, Jones OR, Rebke M (2012) BaSTA: An R package for Bayesian estimation of age-specific survival from incomplete mark-recapture/recovery data with covariates. *Methods Ecol Evol* 3:466–470.
64. Colchero F, Clark JS (2012) Bayesian inference on age-specific survival for censored and truncated data. *J Anim Ecol* 81(1):139–149.
65. Siler W (1979) A competing-risk model for animal mortality. *Ecology* 60(4):750–757.
66. Metropolis N, Rosenbluth AW, Rosenbluth MN, Teller AH, Teller E (1953) Equation of state calculations by fast computing machines. *J Chem Phys* 21(6):1087–1092.
67. Clark JS (2007) *Models for Ecological Data: An Introduction* (Princeton Univ Press, Princeton).
68. Durbin J, Watson GS (1950) Testing for serial correlation in least squares regression. I. *Biometrika* 37(3-4):409–428.
69. Pagel M (1999) Inferring the historical patterns of biological evolution. *Nature* 401(6756):877–884.
70. Arnold C, Matthews LJ, Nunn CL (2010) The 10kTrees website: A new online resource for primate phylogeny. Evol Anthropol Issues *News Rev* 19(3):114–118.
71. Bininda-Emonds ORP, et al. (2007) The delayed rise of present-day mammals. *Nature* 446(7135):507–512.
72. R Core Team (2015) *R: A Language and Environment for Statistical Computing* (R Foundation for Statistical Computing Vienna).
73. Jierong L, Ruyong S (1985) Studies on the life table and reproduction of the root vole Microtus oeconomus. *Acta Zoologica Sinica* 31(2):170–177.
74. Schwartz OA, Armitage KB, Van Vuren D (1998) A 32-year demography of yellow-bellied marmots (Marmota flaviventris). *J Zool* 246(3):337–346.
75. Tryon CA, Snyder DP (1973) Biology of the eastern chipmunk, Tamias striatus: Life tables, age distributions, and trends in population numbers. *J Mammal* 54(1):145–168.
76. Spinage CA (1972) African ungulate life tables. *Ecology* 53(4):645–652.
77. Wolfe ML (1977) Mortality patterns in the Isle Royale moose population. *Am Midl Nat* 97(2):267–279.
78. Tokida K, Miura S (1988) Mortality and life table of a Japanese serow (Capricornis crispus) population in Iwate prefecture, Japan. *J Mammal Soc Jpn* 13(2):119–126.
79. Ahrestani FS, Iyer S, Heitkönig IMA, Prins HHT (2011) Life-history traits of gaur Bos gaurus: A first analysis. *Mammal Rev* 41(1):75–84.
80. Comfort A, Matthews LH (1956) Longevity and mortality of Irish wolfhounds. *Proc Zool Soc Lond* 127(1):27–34.